

# $K^0$ and $K^+$ -meson electromagnetic form factors: a nonperturbative relativistic quark model versus experimental, perturbative and lattice Quantum-Chromodynamics results

S.V. Troitsky<sup>1,\*</sup> and V.E. Troitsky<sup>2,†</sup>

<sup>1</sup>*Institute for Nuclear Research of the Russian Academy of Sciences,  
60th October Anniversary Prospect 7a, Moscow 117312, Russia*

<sup>2</sup>*D.V. Skobeltsyn Institute of Nuclear Physics,  
M. V. Lomonosov Moscow State University, Moscow 119991, Russia*

It has been previously shown that a particular nonperturbative constituent-quark model of hadrons describes experimental measurements of electromagnetic form factors of light charged mesons through a small number of common phenomenological parameters, matching at the same time the Quantum-Chromodynamics (QCD) asymptotics for the  $\pi$ -meson form factor at large momentum transfer. Here we start with the determination of the  $K^0$  electromagnetic form factor in this approach. Precise measurement of the  $K^0$  charge radius makes it possible to constrain model parameters with high accuracy. Then, with all parameters fixed, we revisit the  $K^+$  form factor and find that it matches experimental measurements in the infrared, lattice results at moderate momentum transfer and the perturbative QCD asymptotics in the ultraviolet. In this way we obtain a narrow constraint on the  $K^+$  charge radius,  $\langle r_{K^+}^2 \rangle = 0.403_{-0.006}^{+0.007} \text{ fm}^2$ , and extend the successful infrared-ultraviolet connection from  $\pi$  to  $K$  mesons.

## I. INTRODUCTION AND OUTLINE

Quantitative description of strongly coupled composite systems remains one of the principal unsolved problems in particle physics. In Quantum Chromodynamics (QCD), perturbative methods fail at low energies, where this gauge theory of strong interactions becomes strongly coupled. The key questions regarding the structure of hadrons and the origin of their masses remain unanswered, see e.g. Ref. [1]. Beyond QCD, the same questions arise in numerous extensions of the Standard Model (SM) of particle physics which predict composite particles bound by new strong gauge forces. Testable first-principle quantitative predictions of these models can only be obtained through lattice calculations, which are however resource consuming. Most of detailed lattice calculations of phenomenological importance are concentrated on the QCD case and are not directly applicable to various beyond-SM theories. It is therefore important to develop novel, ready to use quantitative approaches to the description of strongly coupled particle bound states, even those applicable to particular problems only. Predictions obtained within these approaches can be tested on QCD, where experimental results are available.

These methods are however not abundant since they need to be fully non-perturbative and have to link parameters of the fundamental theory, defined at weak coupling (ultraviolet), to observables defined at strong coupling (infrared). The present work aims to contribute to the development of one of such methods.

The approach we follow makes use of a constituent-quark model which keeps relativistic invariance at every

step of calculations. This nonperturbative method [2–4] is based on Dirac Relativistic Hamiltonian Dynamics, see e.g. Ref. [5], in its instant form. Relativistic invariance is guaranteed by the use of modified impulse approximation [2]. The model was used to calculate the electromagnetic form factor,  $F_\pi$ , of the  $\pi$  meson as a function of squared momentum transfer,  $Q^2$ , with a small number of parameters as early as in 1998 [6]. Subsequent measurements [7] of  $F_\pi(Q^2)$  matched the model predictions perfectly [8].

At large  $Q^2$ , when the constituent-quark masses are switched off,  $F_\pi(Q^2)$  calculated in the model agrees with the perturbative QCD prediction [9–11], both in the functional form [12] and numerically [13]. This is remarkable because the correct ultraviolet asymptotics is reached automatically for the same choice of parameters which describes infrared data.

Further studies within this approach included calculations of electromagnetic properties of other light mesons [14, 15], as well as preliminary studies of the  $\pi$ -meson gravitational form factor [16] and a generalization of the infrared-ultraviolet  $\pi$ -meson link to gauge theories beyond QCD [17], in a general agreement with available lattice results. However, one of parameters of the model for  $K$  mesons remained poorly constrained because of the low precision of the experimental determination of  $K^+$  charge radius,  $\langle r_{K^+}^2 \rangle^{1/2}$ . In Ref. [15], we presented the allowed range for the  $K^+$  form factor,  $F_{K^+}(Q^2)$ , and pointed out that more data are necessary to obtain firm predictions. In particular, no conclusive study of the ultraviolet behaviour of  $F_{K^+}(Q^2)$  was possible with that level of precision.

The present work fills this gap and makes use of much more precise experimental measurements of the  $K^0$  charge radius,  $\langle r_{K^0}^2 \rangle^{1/2}$ . The calculation of the  $K^0$  electromagnetic form factor is a straightforward generalization of that for  $K^+$ , and  $F_{K^0}(Q^2)$  is determined

\* st@ms2.inr.ac.ru

† troitsky@theory.sinp.msu.ru

by the same set of parameters. In Sec. II, we use the measurement of  $\langle r_{K^0}^2 \rangle^{1/2}$  to remove the freedom in the only unconstrained parameter and make firm predictions for  $F_{K^0}(Q^2)$ . With all parameters fixed in this way, in Sec. III we calculate and explore  $F_{K^+}(Q^2)$ . Its behaviour at  $Q^2 \rightarrow 0$  determines the  $K^+$  charge radius, which we constrain to a very narrow range. The precision is now sufficient to demonstrate the agreement with recent lattice calculations of  $F_{K^+}(Q^2)$  at  $Q^2 \sim$  a few  $\text{GeV}^2$  and to determine unambiguously the asymptotics  $F_{K^+}(Q^2 \rightarrow \infty)$ , which we find to agree precisely with the perturbative QCD prediction. Section IV summarizes main results of this work, stressing in particular the importance of the obtained extension of the quantitative infrared-ultraviolet connection from  $\pi$  to  $K$  mesons.

## II. $K^0$ FORM FACTOR AND PARAMETER FIXING

General formalism and particular formulae for calculation of meson electromagnetic form factors have been presented in previous publications [2, 6, 8, 15, 18], see in particular Appendix A of Ref. [15] for the  $K^+$  meson; expressions for  $K^0$  are obtained by a simple substitution of  $u$  to  $d$  quark charges and magnetic moments. To calculate the electromagnetic form factor of a meson in our approach, one has to fix the following parameters (see also Table I in Sec. IV):

- masses  $M_{q_1, q_2}$  of two constituent quarks  $q_1, q_2$  composing the meson;
- wave-function confinement scale  $b$ ;
- values  $\kappa_{q_1, q_2}$  of anomalous magnetic moments of the two quarks.

The values of  $\kappa_{u, d, s}$  are determined a priori from model-independent sum rules [19], see Ref. [15] for more details, so they are not treated as free parameters. Here, we use the most recent data from Ref. [20] to reevaluate  $\kappa_s$  and its uncertainties. Also, the value of the light-quark constituent mass,  $M_u = M_d = 0.22 \text{ GeV}$ , was determined with high accuracy in previous studies of the  $\pi$ -meson form factor (this value was motivated also in Ref. [21] on different grounds). Given the precision of measurement of  $\pi$ -meson related quantities, their contribution to the error balance is expected to be small compared to the  $K$ -meson ones. We are left with two parameters for the  $K$  mesons,  $M_s$  and  $b$ . One combination of them is determined from the requirement of reproducing the correct experimental value of the meson decay constant  $f_K$ , cf. Refs. [15, 22], and the only remaining parameter is subject to fit. Previous studies of the  $\pi$  and  $K^+$  mesons used lower-energy measurements of the meson charge radius to fix it. While for the  $\pi$  meson this was sufficient to determine the behaviour of  $F_\pi(Q^2)$  for all  $Q^2$  and even to prove that the correct asymptotics is reached at  $Q^2 \rightarrow 0$  if  $M_u$  is switched off [13], precision of available measurements of  $\langle r_{K^+}^2 \rangle^{1/2}$  is too low to make firm conclusions even at moderate  $Q^2$ . In Ref. [15], we determined the

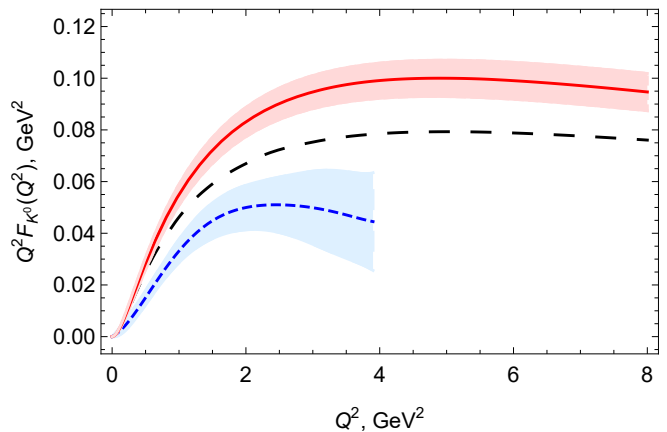


FIG. 1. Results of the present work for the neutral kaon form factor (full red line with light-red shadow uncertainty region) compared to the lattice results [24] (dashed blue line with light-blue uncertainty region) and the calculation of Ref. [25] (long-dashed black line).

range of available values of  $F_{K^+}(Q^2)$  and noted that future experiments, even at moderate  $Q^2$ , will constrain the  $K^+$  charge radius in this approach.

The confinement scale  $b$  deserves some comments. First, its definition depends on the particular choice of the meson wave function, but it has been shown [6] (see also Ref. [23]) that the result for the form factor does not depend on this choice, provided the parameters are fixed in such a way that the correct decay constant is reproduced. Here we use the same parametrisation of the wave function as in Ref. [15]. Second, though the direct derivation of  $b$  in terms of underlying theory is not available, one expects that its value is determined by masses and strong-interaction properties of the two quarks composing the meson. Therefore, the values of  $b$  are different for  $\pi$  and  $K$  but are expected to be the same for  $K^+$  and  $K^0$ . This makes it possible to use  $f_K$  and either  $\langle r_{K^0}^2 \rangle$  or  $\langle r_{K^+}^2 \rangle$  to constrain  $M_s$  and  $b$  required for derivation of both  $F_{K^+}(Q^2)$  and  $F_{K^0}(Q^2)$ . Self-consistency of this approach will be checked with the asymptotics of  $F_{K^+}(Q^2)$  in Sec. III.

We use the values of  $f_K = 0.1562 \pm 0.0010 \text{ GeV}$  (same as in Ref. [15] for consistency; more recent estimates [20] coincide with it within error bars) and of  $\langle r_{K^0}^2 \rangle = -0.077 \pm 0.010 \text{ fm}^2$  [20] to find  $M_s = 0.3177 \pm 0.0040 \text{ GeV}$  and  $b = 0.7118 \mp 0.0050 \text{ GeV}$  (error bars of  $b$  and  $M_s$  are correlated). Figure 1 presents  $F_{K^0}(Q^2)$  for these parameters in comparison with the lattice result [24] and with theoretical calculations of Ref. [25]. A certain disagreement with the lattice result is explained by the fact that the lattice calculation [24] does not reproduce the experimental value of the  $K^0$  charge radius to which we tuned our parameters: as it has been pointed out in Ref. [1], the lattice value is  $\langle r_{K^0}^2 \rangle \approx -0.026 \text{ fm}^2$ , far beyond the experimental error bars.

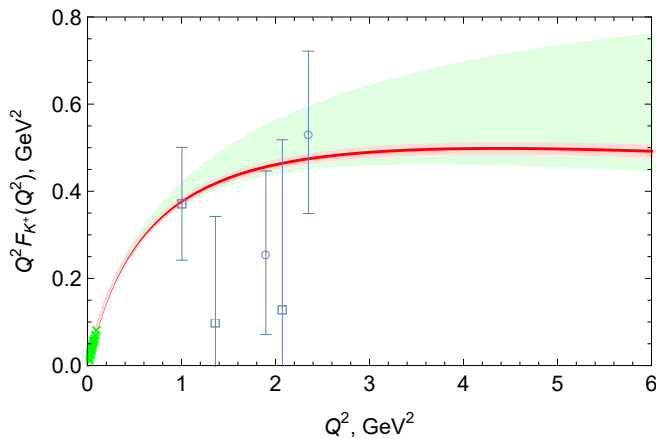


FIG. 2. Results of the present work for the charged kaon form factor (full red line with light-red shadow uncertainty region), with parameters fixed from  $K^0$  charge radius, compared to our previous work [15] (light-green shading), where the parameters were constrained from the  $K^+$  charge radius. Experimental measurements: green crosses at  $Q^2 \rightarrow 0$ , NA7 [26]; squares, E93-018 [27]; circles, E98-108 [27].

### III. $K^+$ FORM FACTOR FROM INFRARED TO ULTRAVIOLET

With all parameters fixed in Sec. II, we proceed to calculate the form factor of  $K^+$ . This repeats the calculation of Ref. [15] but with all remaining freedom restricted to tiny error bars in  $M_s$  and  $b$  specified in Sec. II. The resulted  $F_{K^+}(Q^2)$  is compared to our previous work [15] in Fig. 2. The change in the precision is dramatic. Figure 3 compares our result for  $F_{K^+}(Q^2)$  with other theoretical calculations.

Since the function  $F_{K^+}(Q^2)$  is predicted without any freedom and with small uncertainties, it is interesting to study its behaviour in more detail. First, we note that at  $Q^2 \rightarrow 0$  it fits experimental measurements [26]. To be more precise in this statement, we obtain the value of the charged kaon charge radius predicted in our approach,  $\langle r_{K^+}^2 \rangle = 0.403^{+0.007}_{-0.006} \text{ fm}^2$  (68% CL). Figure 4 presents a graphical comparison of this value with the experimental determination of  $\langle r_{K^+}^2 \rangle$  [26], our previous constraints [15] and lattice results [37]. We note that the value of  $\langle r_{K^+}^2 \rangle$  obtained in the present work agrees well with all these previous results, while the precision is improved considerably. It also agrees with less precise predictions of chiral perturbation theory [38] and of a holographic light-front model [39].

Let us move now to moderate  $Q^2$  of order a few  $\text{GeV}^2$ . Presently, there are no precise experimental measurements of  $F_{K^+}(Q^2)$  in this range, so we compare our result to those of the lattice QCD calculation [24]; Fig. 3 demonstrates a good agreement (we will return to the lattice comparison in Sec. IV). Measurements of  $F_{K^+}(Q^2)$  at the Jefferson Laboratory [40, 41] and the Electron-Ion Collider [42] will make it possible to test our predictions

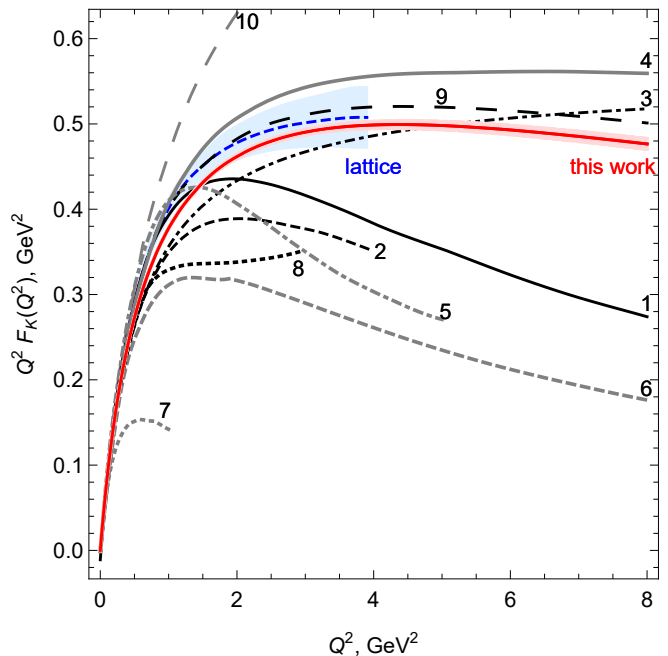


FIG. 3. Results of the present work for the charged kaon form factor (full red line with light-red shadow uncertainty region) compared to the lattice results [24] (dashed blue line with light-blue uncertainty region) and other theoretical studies — 1 (full black): Ref. [28]; 2 (dashed black): Ref. [29]; 3 (dot-dashed black): Ref. [30]; 4 (full gray): Ref. [31]; 5 (dot-dashed gray): Ref. [32]; 6 (dashed gray): Ref. [33]; 7 (dotted gray): Ref. [34]; 8 (dotted black): Ref. [35]; 9 (long-dashed black): Ref. [25]; 10 (long-dashed gray): Ref. [36].

experimentally.

We turn now to the asymptotic regime,  $Q^2 \rightarrow \infty$ . A way to merge the regime of relativistic constituent-quark models,  $Q^2 \rightarrow 0$ , and that of the perturbative QCD,  $Q^2 \rightarrow \infty$ , is to allow the quark mass to run from the constituent-quark mass  $M$  in the infrared to the current-quark mass  $m \ll M$  in the ultraviolet, see e.g. Ref. [43]. This implies switching off constituent-quark masses in the asymptotic regime. Within our approach, switching the mass off resulted [12] in the correct functional form of  $F_\pi(Q^2 \rightarrow \infty)$  in agreement with QCD predictions [44, 45]. Moreover, we have shown [13] that no matter how the masses are switched off, the correct coefficient of the perturbative QCD asymptotics of  $F_\pi$  [9–11] is properly reproduced. Since all parameters of the model are fixed in the low- $Q^2$  limit, this provides a nontrivial infrared–ultraviolet link yet to be understood in a fundamental theory. Extension of this approach to other gauge theories beyond QCD [17] resulted in a reasonable agreement with scarce available lattice calculations. Here we make use of the precise parameter-free prediction of  $F_{K^+}(Q^2)$  to test whether this unusual result holds for the mesons other than  $\pi$ .

We follow the approach discussed in detail in Ref. [13]. We choose the same family of functions  $M(Q^2)$ , see

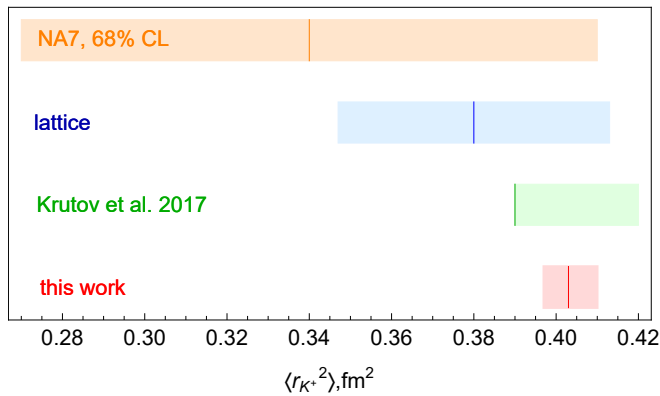


FIG. 4.  $K^+$  charge radius as determined by the NA7 experiment in CERN [26] (error bars scaled from reported 50% CL to 68% CL assuming Gaussian distribution), by lattice calculations [37], by a fit of Ref. [26] data in our model (Krutov et al. 2017, Ref. [15]) and by making use of constraints from  $\langle r_{K^0}^2 \rangle$  in the present work.

Sec. II.B of Ref. [13], motivated by Refs. [43, 46], which describe switching constituent-quark masses off at high  $Q^2$ . The functional shapes for  $M_{u,d}(Q^2)$  and  $M_s(Q^2)$  are the same, while their values at  $Q^2 = 0$  are fixed as described above. This implies in particular that  $M(Q^2) \simeq M(0)$  for  $Q^2 \lesssim 8 \text{ GeV}^2$ , the range to be tested in coming experiments. We vary two parameters of  $M(Q^2)$  shape, which describe where and how smoothly the mass is turned off. In a complete analogy with what we observe for  $F_\pi(Q^2)$  in Ref. [13], cf. Fig. 4 of that work, we find that  $F_{K^+}(Q^2 \rightarrow \infty)$  does not depend on these two parameters. Note that the behaviour of  $F_{K^+}(Q^2)$  in the transition region, before the asymptotics is reached, depends on the choice of the  $M(Q^2)$  function.

We are now ready to answer the most intriguing question, whether our approach reproduces the correct QCD asymptotics for  $F_{K^+}(Q^2)$  like it does for  $F_\pi(Q^2)$ . The asymptotics, determined in Ref. [11], reads

$$F_{K^+}(Q^2 \rightarrow \infty) \sim F_{K^+}^{\text{as}} = \frac{8\pi}{Q^2} f_K^2 \alpha_S^{1-\text{loop}}(Q^2), \quad (1)$$

where  $\alpha_S^{1-\text{loop}}(Q^2)$  is one-loop running strong gauge coupling constant.

The correct  $Q^2$  dependence of the form factor is guaranteed, for  $M = 0$ , by analytical calculations of Ref. [12]. We need to calculate the coefficient numerically to compare it with that given by Eq. (1). We start with the strong coupling at the  $Z$ -boson mass scale,  $\alpha_S(Q^2 = M_Z^2) = 0.1187 \pm 0.0018$  [20], and evolve it down with the one-loop renormalization-group equation for QCD with  $N_f = 5$  flavours. The uncertainty in Eq. (1) comes from a combination of experimental error bars of  $\alpha_S(M_Z^2)$  and the intrinsic theoretical uncertainty behind the one-loop expression (1). The latter is not straightforward to estimate since the generalization of Eq. (1) to the second loop is nontrivial. To estimate the theoretical uncertainty in Eq. (1), we loosely assume that it is of order of the

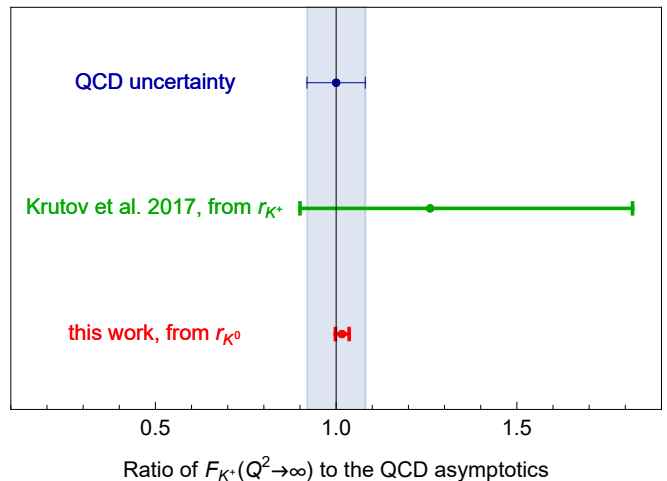


FIG. 5. Ratio of the asymptotics of  $F_{K^+}(Q^2 \rightarrow \infty)$ , obtained in our model after switching off quark masses, to the perturbative QCD asymptotics [47]. Note that the correct functional form is obtained automatically in our approach, and this plot presents the ratio of the coefficients constrained in the previous study (Krutov et al. 2017, Ref. [15]) and by making use of constraints from  $\langle r_{K^0}^2 \rangle$  in the present work. See the text for the estimate of the QCD uncertainty.

ratio of the second and first loop contributions to the beta function; summed up in quadratures with the uncertainty in  $\alpha_S(M_Z^2)$ , this gives about 8% estimated QCD uncertainty at  $Q_0^2 \sim 200 \text{ GeV}^2$ . The ratio of  $F_{K^+}(Q_0^2)$ , calculated in our approach, to the asymptotics (1) for  $\alpha_S(M_Z^2) = 0.1187$  gives

$$F_{K^+}/F_{K^+}^{\text{as}} \simeq 1.016_{-0.018}^{+0.020},$$

well within the  $1.00 \pm 0.08$  QCD uncertainty (see Fig. 5). This remarkable agreement extends our successful infrared-ultraviolet link of  $F_\pi$  [13, 17] to the  $K$ -meson form factors.

#### IV. DISCUSSION AND CONCLUSIONS

We have calculated the neutral kaon electromagnetic form factor within the same model and through the same parameters as it was previously done for the charged kaon [15]. This has allowed us to fix the remaining uncertain parameter of the model through the  $K^0$  charge radius, which is measured with much better precision than that of  $K^+$ . As a result, we calculated also  $F_{K^+}(Q^2)$  with very small uncertainty, see Figs. 2, 3, and without any remaining freedom in parameters, cf. Table I. At  $Q^2 \rightarrow 0$ , this calculation matches experimental and lattice results for the  $K^+$  charge radius, at the same time predicting its value with much higher precision, cf. Fig. 4. The values of the form factors calculated in this work are given in Table II in Appendix A together with their uncertainties.

TABLE I. Inputs and outputs of the present work. See Ref. [15] for details and the text for references concerning the fixed parameters.

Fixed parameters	light-quark constituent mass	$M_u \equiv M_d = 0.22 \text{ GeV}$	} Fixed from previous $\pi$ -meson studies
	quark anomalous magnetic moments	$\kappa_u = -0.01055$ $\kappa_{\bar{d}} = 0.03735$ $\kappa_{\bar{s}} = -0.084 \pm 0.019$	
Fitted parameters	strange-quark constituent mass	$M_s = 0.3177 \pm 0.0040 \text{ GeV}$	Fitted here from measured $f_K$ and $\langle r_{K^0}^2 \rangle$
	$K$ -meson wave-function scale	$b = 0.7118 \mp 0.0050 \text{ GeV}$	
Outputs	Form factors $F_{K^0}(Q^2)$ , $F_{K^+}(Q^2)$	$Q^2 \rightarrow 0$ : refined $\langle r_{K^+}^2 \rangle$ , matches measurements $Q^2 \sim \text{few GeV}^2$ : matches lattice calculations $Q^2 \rightarrow \infty$ : matches the perturbative QCD asymptotics	

At moderate  $Q^2 \lesssim 4 \text{ GeV}^2$ , we compare our results for  $F_{K^0, K^+}(Q^2)$  with lattice QCD calculations of Ref. [24], see Figs. 1, 3. Our  $F_{K^+}(Q^2)$  agrees very well with the lattice result, while the agreement is much worse for  $F_{K^0}(Q^2)$ . This is not surprising since the lattice result does not reproduce the measured  $K^0$  charge radius, which we used to fit the key parameter of our model. In a deeper context, this disagreement may be related to the fact that the lattice  $K^0$  form factor was obtained as a difference between contributions from two quarks, weighted by their charges. We note that in our approach, electromagnetic properties of the quarks differ not only by their charges but also by their anomalous magnetic moments; form factors of  $K^0$  and  $K^+$  are therefore not decomposed into charge-weighted linear combinations of contributions from each quark. The contribution of the anomalous magnetic moments is  $\sim 6\%$  for  $K^+$  while for  $K^0$ , it exceeds  $\sim 50\%$ . This explains in particular the fact that  $F_{K^+}(Q^2)$  agrees with the lattice results while  $F_{K^0}(Q^2)$  does not agree, which is also the case for the results of Refs. [1, 25].

At  $Q^2 \rightarrow \infty$ , upon switching constituent-quark masses off,  $F_{K^+}(Q^2)$  reaches precisely the perturbative QCD asymptotics, cf. Fig. 5. This is achieved without any parameter tuning: all free parameters of the model are fixed in the infrared. This is similar to the behaviour of  $F_\pi(Q^2)$  found previously in our approach: the asymptotics are different but both are achieved automatically. Our calculation does not predict the scale of the momentum transfer at which the transition to the perturbative regime happens: it is related to the scale at which  $M(Q^2)$

goes to zero; but the correct asymptotics is reached independently of that scale. This scale, predicted to be as low as  $Q^2 \simeq 3.5 \text{ GeV}^2$  for  $F_\pi$  [48], is probably actually higher, as it is suggested by measurements of  $F_\pi(Q^2)$  [7] and lattice calculations of  $F_{K^+}(Q^2)$  [24]. To determine this scale in our model, further experimental input is required [49]. However, the relations between infrared and ultraviolet properties of the form factors are valid independently of their behaviour at moderate  $Q^2$ . This makes it possible to apply these relations in new-physics models with strongly-coupled gauge theories [17]. In particular, these include models with composite Higgs and dark-matter particles, see e.g. Refs. [50, 51]: there, the low- $Q^2$  form factor of a neutral meson-like state, similar to  $K^0$ , determines observable properties relevant for the dark-matter search. This avenue will be explored elsewhere.

### Appendix A: Numerical results for the $K^0$ and $K^+$ form factors

Table II presents the form factors  $F_{K^0}(Q^2)$ ,  $F_{K^+}(Q^2)$ , determined in this work, in the numerical form.

### ACKNOWLEDGMENTS

This research has been supported by the Interdisciplinary Scientific and Educational School of Moscow University ‘‘Fundamental and Applied Space Research’’. We thank A. Krutov for fruitful discussions. ST thanks A. Kataev for bringing  $K^0$  results to his attention.

[1] C. D. Roberts, D. G. Richards, T. Horn and L. Chang, ‘‘Insights into the Emergence of Mass from Studies of

Pion and Kaon Structure,’’ [arXiv:2102.01765 [hep-ph]].

TABLE II. Values of  $K^0$  and  $K^+$  electromagnetic form factors obtained in this work.

$Q^2$ , GeV <sup>2</sup>	$F_{K^0}$	$F_{K^+}$
0.0	0.0000 ± 0.0000	1.0000 + 0.0000 − 0.0000
0.1	0.0262 ± 0.0029	0.8509 + 0.0006 − 0.0006
0.2	0.0412 ± 0.0041	0.7444 + 0.0009 − 0.0009
0.3	0.0497 ± 0.0046	0.6628 + 0.0012 − 0.0012
0.4	0.0544 ± 0.0048	0.5978 + 0.0014 − 0.0013
0.5	0.0567 ± 0.0047	0.5447 + 0.0015 − 0.0015
0.6	0.0576 ± 0.0047	0.5003 + 0.0016 − 0.0015
0.7	0.0576 ± 0.0045	0.4626 + 0.0017 − 0.0016
0.8	0.0571 ± 0.0044	0.4302 + 0.0018 − 0.0017
0.9	0.0562 ± 0.0042	0.4019 + 0.0018 − 0.0017
1.0	0.0550 ± 0.0041	0.3770 + 0.0019 − 0.0018
1.5	0.0481 ± 0.0034	0.2871 + 0.0021 − 0.0019
2.0	0.0416 ± 0.0028	0.2305 + 0.0021 − 0.0020
2.5	0.0361 ± 0.0024	0.1916 + 0.0022 − 0.0020
3.0	0.0316 ± 0.0021	0.1631 + 0.0022 − 0.0020
3.5	0.0279 ± 0.0019	0.1415 + 0.0022 − 0.0020
4.0	0.0248 ± 0.0017	0.1244 + 0.0021 − 0.0020
4.5	0.0222 ± 0.0015	0.1107 + 0.0021 − 0.0019
5.0	0.0200 ± 0.0014	0.0994 + 0.0021 − 0.0019
5.5	0.0181 ± 0.0013	0.0900 + 0.0020 − 0.0018
6.0	0.0165 ± 0.0012	0.0820 + 0.0020 − 0.0018
6.5	0.0151 ± 0.0011	0.0751 + 0.0019 − 0.0017
7.0	0.0139 ± 0.0010	0.0692 + 0.0017 − 0.0016
7.5	0.0128 ± 0.0010	0.0640 + 0.0017 − 0.0015
8.0	0.0118 ± 0.0009	0.0594 + 0.0016 − 0.0014

- [2] A. F. Krutov and V. E. Troitsky, “Relativistic instant form approach to the structure of two-body composite systems,” *Phys. Rev. C* **65** (2002) 045501 [hep-ph/0204053].
- [3] A. F. Krutov and V. E. Troitsky, “Relativistic instant form approach to the structure of two-body composite systems. 2. Nonzero spin,” *Phys. Rev. C* **68** (2003) 018501 [hep-ph/0210046].
- [4] A. F. Krutov and V. E. Troitsky, “Instant form of Poincare-invariant quantum mechanics and description of the structure of composite systems,” *Phys. Part. Nucl.* **40** (2009) 136.
- [5] B. D. Keister and W. N. Polyzou, “Relativistic Hamiltonian dynamics in nuclear and particle physics,” *Adv. Nucl. Phys.* **20** (1991) 225.
- [6] A. F. Krutov and V. E. Troitsky, “On a possible estimation of the constituent quark parameters from Jefferson Lab experiments on pion form-factor,” *Eur. Phys. J. C* **20** (2001) 71 [hep-ph/9811318].
- [7] G. M. Huber *et al.* [Jefferson Lab Collaboration], “Charged pion form-factor between  $Q^2 = 0.60$  GeV<sup>2</sup> and 2.45 GeV<sup>2</sup>. II. Determination of, and results for, the pion form-factor,” *Phys. Rev. C* **78** (2008) 045203 [arXiv:0809.3052 [nucl-ex]].
- [8] A. F. Krutov, V. E. Troitsky and N. A. Tsirova, “Non-perturbative relativistic approach to pion form factor versus JLab experiments,” *Phys. Rev. C* **80** (2009) 055210 [arXiv:0910.3604 [nucl-th]].
- [9] G. R. Farrar and D. R. Jackson, “The Pion Form-Factor,” *Phys. Rev. Lett.* **43** (1979) 246
- [10] A. V. Efremov and A. V. Radyushkin, “Factorization and Asymptotical Behavior of Pion Form-Factor in QCD,” *Phys. Lett. B* **94** (1980) 245
- [11] G. P. Lepage and S. J. Brodsky, “Exclusive Processes in Quantum Chromodynamics: Evolution Equations for Hadronic Wave Functions and the Form-Factors of Mesons,” *Phys. Lett. B* **87** (1979) 359
- [12] A. F. Krutov and V. E. Troitsky, “Asymptotic estimates of the pion charge form-factor,” *Theor. Math. Phys.* **116** (1998) 907 [*Teor. Mat. Fiz.* **116** (1998) 215].
- [13] S. V. Troitsky and V. E. Troitsky, “Transition from a relativistic constituent-quark model to the quantum-chromodynamical asymptotics: a quantitative description of the pion electromagnetic form factor at intermediate values of the momentum transfer,” *Phys. Rev. D* **88** (2013) 093005 [arXiv:1310.1770 [hep-ph]].
- [14] A. F. Krutov, R. G. Polezhaev and V. E. Troitsky, “The radius of the  $\rho$  meson determined from its decay constant,” *Phys. Rev. D* **93** (2016) 036007 [arXiv:1602.00907 [hep-ph]].
- [15] A. F. Krutov, S. V. Troitsky and V. E. Troitsky, “The  $K$ -meson form factor and charge radius: linking low-energy data to future Jefferson Laboratory measurements,” *Eur. Phys. J. C* **77** (2017) 464 [arXiv:1610.06405 [hep-ph]].
- [16] A. F. Krutov and V. E. Troitsky, “Pion gravitational form factors in a relativistic theory of composite particles,” *Phys. Rev. D* **103** (2021) 014029 [arXiv:2010.11640 [hep-ph]].
- [17] S. Troitsky and V. Troitsky, “Linking infrared and ultraviolet parameters of pion-like states in strongly coupled gauge theories,” *Eur. Phys. J. C* **78** (2018) 899 [arXiv:1807.11009 [hep-ph]].
- [18] E. V. Balandina, A. F. Krutov and V. E. Troitsky, “Elastic charge form-factors of  $\pi$  and  $K$  mesons,” *J. Phys. G* **22** (1996) 1585 [hep-ph/9508248].
- [19] S. B. Gerasimov, “Electroweak moments of baryons and hidden strangeness of the nucleon,” *Chin. J. Phys.* **34** (1996) 848 [hep-ph/9906386].
- [20] P. A. Zyla *et al.* [Particle Data Group], “Review of Particle Physics,” *PTEP* **2020** (2020) 083C01
- [21] S. Godfrey and N. Isgur, “Mesons in a Relativized Quark Model with Chromodynamics,” *Phys. Rev. D* **32** (1985) 189.
- [22] A. F. Krutov, “Electroweak properties of light mesons in the relativistic model of constituent quarks,” *Phys. Atom. Nucl.* **60** (1997) 1305 [*Yad. Fiz.* **60** (1997) 1442].
- [23] F. Schlumpf, “Charge form-factors of pseudoscalar mesons,” *Phys. Rev. D* **50** (1994) 6895 [hep-ph/9406267].
- [24] C. T. H. Davies *et al.* [HPQCD], “Meson Electromagnetic Form Factors from Lattice QCD,” *PoS LATTICE2018* (2018) 298 [arXiv:1902.03808 [hep-lat]].
- [25] F. Gao, L. Chang, Y. X. Liu, C. D. Roberts and P. C. Tandy, “Exposing strangeness: projections for kaon electromagnetic form factors,” *Phys. Rev. D* **96** (2017) 034024 [arXiv:1703.04875 [nucl-th]].
- [26] S. R. Amendolia *et al.*, “A Measurement of the Kaon Charge Radius,” *Phys. Lett. B* **178** (1986) 435.
- [27] M. Carmignotto *et al.*, “Separated Kaon Electroproduction Cross Section and the Kaon Form Factor from 6 GeV JLab Data,” *Phys. Rev. C* **97** (2018) 025204 [arXiv:1801.01536 [nucl-ex]].

- [28] J. He, B. Julia-Diaz and Y. b. Dong, “Electroweak properties of the  $\pi$ ,  $K$  and  $K^*(892)$  in the three forms of relativistic kinematics,” *Eur. Phys. J. A* **24** (2005) 411 [hep-ph/0503294].
- [29] P. Maris and P. C. Tandy, “The  $\pi$ ,  $K^+$ , and  $K^0$  electromagnetic form-factors,” *Phys. Rev. C* **62** (2000) 055204 [nucl-th/0005015].
- [30] Y. Ninomiya, W. Bentz and I. C. Cloet, “Dressed Quark Mass Dependence of Pion and Kaon Form Factors,” *Phys. Rev. C* **91** (2015) 025202 [arXiv:1406.7212 [nucl-th]].
- [31] P. T. P. Hutaeruk, I. C. Cloet and A. W. Thomas, “Flavor dependence of the pion and kaon form factors and parton distribution functions,” *Phys. Rev. C* **94** (2016) 035201 [arXiv:1604.02853 [nucl-th]].
- [32] C. J. Burden, C. D. Roberts and M. J. Thomson, “Electromagnetic form-factors of charged and neutral kaons,” *Phys. Lett. B* **371** (1996) 163 [nucl-th/9511012].
- [33] F. Cardarelli, I. L. Grach, I. M. Narodetsky, E. Pace, G. Salme and S. Simula, “Charge form-factor of pi and K mesons,” *Phys. Rev. D* **53** (1996) 6682 [nucl-th/9507038].
- [34] E. O. da Silva, J. P. B. C. de Melo, B. El-Bennich and V. S. Filho, “Pion and kaon elastic form factors in a refined light-front model,” *Phys. Rev. C* **86** (2012) 038202 [arXiv:1206.4721 [nucl-th]].
- [35] D. Ebert, R. N. Faustov and V. O. Galkin, “Masses and electroweak properties of light mesons in the relativistic quark model,” *Eur. Phys. J. C* **47** (2006) 745 [hep-ph/0511029].
- [36] Z. Abidin and P. T. P. Hutaeruk, “Kaon form factor in holographic QCD,” *Phys. Rev. D* **100** (2019) 054026 [arXiv:1905.08953 [hep-ph]].
- [37] S. Aoki *et al.* [JLQCD Collaboration], “Light meson electromagnetic form factors from three-flavor lattice QCD with exact chiral symmetry,” *Phys. Rev. D* **93** (2016) 034504 [arXiv:1510.06470 [hep-lat]].
- [38] J. Bijnens and P. Talavera, “Pion and kaon electromagnetic form-factors,” *JHEP* **0203** (2002) 046 [hep-ph/0203049].
- [39] M. Ahmady, C. Mondal and R. Sandapen, “Dynamical spin effects in the holographic light-front wavefunctions of light pseudoscalar mesons,” *Phys. Rev. D* **98** (2018) 034010 [arXiv:1805.08911 [hep-ph]].
- [40] J. Dudek *et al.*, “Physics Opportunities with the 12 GeV Upgrade at Jefferson Lab,” *Eur. Phys. J. A* **48** (2012) 187 [arXiv:1208.1244 [hep-ex]].
- [41] T. Horn and C. D. Roberts, “The pion: an enigma within the Standard Model,” *J. Phys. G* **43** (2016) 073001 [arXiv:1602.04016 [nucl-th]].
- [42] J. Arrington *et al.*, “Revealing the structure of light pseudoscalar mesons at the Electron-Ion Collider,” [arXiv:2102.11788 [nucl-ex]].
- [43] L. S. Kisslinger, H. M. Choi and C. R. Ji, “Pion form-factor and quark mass evolution in a light front Bethe-Salpeter model,” *Phys. Rev. D* **63** (2001) 113005 [arXiv:hep-ph/0101053 [hep-ph]].
- [44] V. A. Matveev, R. M. Muradyan and A. N. Tavkhelidze, “Automodelity in strong interactions,” *Lett. Nuovo Cim.* **5S2** (1972) 907
- [45] S. J. Brodsky and G. R. Farrar, “Scaling Laws at Large Transverse Momentum,” *Phys. Rev. Lett.* **31** (1973) 1153
- [46] A. Doff, F. A. Machado and A. A. Natale, “Chiral symmetry breaking in QCD-like gauge theories with a confining propagator and dynamical gauge boson mass generation,” *Annals Phys.* **327** (2012) 1030 [arXiv:1106.2860 [hep-ph]].
- [47] G. P. Lepage and S. J. Brodsky, *Phys. Rev. D* **22** (1980) 2157
- [48] O. C. Jacob and L. S. Kisslinger, “Applicability of Asymptotic {QCD} for Exclusive Processes,” *Phys. Rev. Lett.* **56** (1986) 225
- [49] S. V. Troitsky and V. E. Troitsky, “Constraining scenarios of the soft/hard transition for the pion electromagnetic form factor with expected data of 12-GeV Jefferson Lab experiments and of the Electron-Ion Collider,” *Phys. Rev. D* **91** (2015) 033008 [arXiv:1501.02712 [hep-ph]].
- [50] Y. Wu, T. Ma, B. Zhang and G. Cacciapaglia, “Composite Dark Matter and Higgs,” *JHEP* **11** (2017) 058 [arXiv:1703.06903 [hep-ph]].
- [51] R. Foadi, M. T. Frandsen and F. Sannino, “Technicolor Dark Matter,” *Phys. Rev. D* **80** (2009) 037702 [arXiv:0812.3406 [hep-ph]].